Exploiting long coherent integration times in DVB-T based passive radar systems

Francesca Filippini*, Tatiana Martelli*, Fabiola Colone*, Roberta Cardinali†

* DIET Dept. Sapienza, University of Rome, Rome, Italy
{francesca.filippini, tatiana.martelli, fabiola.colone}@uniroma1.it

† Leonardo Company, Rome, Italy
roberta.cardinali@leonardocompany.com

Abstract — **Long coherent integration times can be exploited in passive radar systems in order to broaden their coverage and to improve their target detection capability. However, proper strategies must be considered to compensate for the target migration effects that could limit the system performance when long coherent processing intervals are used. In this paper, we refer to the case of a passive coherent location system for air traffic surveillance, exploiting DVB-T signals as source of opportunity, and we propose two strategies able to deal with the typically high speeds and possible accelerations of civil aircrafts. We show that the proposed detection schemes allow to effectively correct the target walk effects and therefore to benefit from the extended coherent integration time, while controlling the false alarm rate. The effectiveness is demonstrated on both simulated and real data provided by Leonardo S.p.A. The experimental results clearly show that the proposed approaches allow the coherent integration time to be increased up to a few seconds.**

Keywords— Passive radar, long coherent integration time, range migration, Doppler migration.

I. INTRODUCTION

Over the past two decades, several signal processing strategies have been conceived to improve the performance of passive radar (PR or *passive coherent location* – PCL) technology and to make these systems mature and effective in different scenarios [1], [2]. As is well known, PCL systems exploit illuminators of opportunity (IOs) to perform target detection and localization. Among the considered waveforms of opportunity, digital broadcast IOs, such as the DVB-T, are particularly attractive for PCL purposes, thanks to many advantages, e.g. wide coverage, stationary and thumbtack shaped ambiguity function [3]. However, by relying on sources of opportunity, PCL system coverage might be limited by the radiative characteristics of the exploited transmitter, which is possibly inadequate for radar purposes [4]. To overcome these limitations thus improving the target detection capability, long integration times can be exploited. To this end, both coherent and non-coherent integrations can be considered [5]-[9]. Typically, in order to limit the computational complexity of the required signal processing techniques, the coherent integration time (CIT or *coherent processing interval* – CPI) is carefully selected to avoid range and Doppler walk effects for the targets of interest [8], whose severity depends on the considered surveillance application as well as on the exploited IO.

In this work, we refer to a DVB-T based PCL system for air traffic surveillance. The coherent integration time typically employed in the considered application to avoid target range/Doppler walk is in the order of one-tenth of a second. Therefore, proper strategies must be considered to take into account the migrations effects arising when increasing the integration time. For the considered application, due to the typical speed of the targets of interest and to the bistatic range resolution of approx. 40 m, the tightest constraint to the CPI is due to the linear range walk effect. This issue has been addressed in the literature and different strategies have been proposed to counteract the problem. The authors presented in [8] a low cost approach by resorting to an efficient implementation of the Keystone Transform (KT) [10] based on Lagrange P-order polynomial interpolation. The effectiveness of the proposed approach was also shown for maritime surveillance [9]. However, the analysis in [8] was mainly focused on targets with a dominant radial velocity component.

In this manuscript, we extend the work in [8], using CPIs up to a few seconds on targets with both radial and tangential velocity components. In this case, solely compensating for the range walk is no longer sufficient in order to benefit from the coherent integration and a Doppler migration (DM) compensation stage is required. Based on two different target search strategies, we propose two alternative detection schemes able to provide the sought correction of walk effects and, consequently, an increased capability to detect migrating targets while appropriately controlling the false alarm rate and the complexity of the resulting architecture.

The proposed solutions are first validated on simulated data, then, their effectiveness is investigated on real data provided by Leonardo S.p.A. The experimental results show that the proposed approaches are suitable for the considered application and allow a significant enhancement of the system coverage thanks to the use of an extended CPI up to a few seconds.

The remainder of this manuscript is organized as follows. In Section II, we summarize the problem while in Section III we describe the two proposed detection strategies and their effectiveness is investigated against simulated data. Then, in Section IV an experimental validation is carried out against real data. Some conclusions are drawn in Section V.

II. PROBLEM FORMULATION

According to a basic DVB-T based PCL processing scheme, the main stages to be performed are (i) stationary disturbance removal at the surveillance channel (ii) evaluation of the bistatic range – bistatic velocity cross ambiguity function (CAF) between the surveillance signal and the reference signal. It is well known that, if the target echoes collected within the CPI remain within the same resolution cell, the CAF evaluation yields a coherent integration gain equal to the number of integrated samples N_s, where $N_s = T \cdot f_s$, f_s is the Nyquist sampling frequency and T is the employed CPI. To guarantee this constraint and to control the computational burden at the receiver, T is typically selected as $T \leq \overline{T} = \min\{\overline{T}^{(R)}, \overline{T}^{(D)}\}$, with $\overline{T}^{(R)}$ and $\overline{T}^{(D)}$ being the maximum CPI allowed without experiencing range and Doppler walk effects, respectively.

In fact, when exploiting a CPI higher than $\overline{T}$, the lack of target migration compensation will cause the final target response to be smeared. This might yield a significant signal-to-noise ratio (SNR) loss on the target peak with respect to its theoretical expectation and possible masking effects from the target energy wandering around the cell under test. This is clearly shown in Fig. 1, where we report an enlarged view of the bistatic range-velocity map obtained after a conventional CAF evaluation with $T = 2s$ for a point-like target echo migrating both in range and in Doppler. Specifically, in the considered example, the receiver is located in the origin of the axes, the transmitter position is $\boldsymbol{P}_{Tx} = [-10 \text{ km}, 0]^T$ and the target moves with constant velocity so that its position can be described by the linear law $\boldsymbol{P}_{TGT}(t) = \boldsymbol{P}_{TGT}(0) + \boldsymbol{v}t$ ($t \in [-T/2, T/2]$, where $\boldsymbol{P}_{TGT}(0) = [15 \text{ km}, 0]^T$ and $\boldsymbol{v} = [60, 80]$ m/s. As is apparent, the target moves along a direction $\varphi = \text{atan}\left(\frac{v_x}{v_y}\right) \approx 53.1°$ with respect to the x axis thus showing motion components both along the bistatic angle (bistatic radial components) and orthogonal to the bistatic angle (cross-range components).

Consequently, the target response in Fig. 1, occupies multiple range and Doppler bins yielding a SNR loss of approx. 14.2 dB, evaluated as the difference between the maximum expected coherent integration gain (72.58dB) and the obtained value. An extensive analysis on the SNR losses of the target peak versus the CPI is reported in Fig. 2 for the severe scenario of a high velocity target, i.e. $\|\boldsymbol{v}\| = 200$ m/s, quite close to the receiver ($\boldsymbol{P}_{TGT}(0) = [5 \text{ km}, 0]^T$).

Specifically, the red curve reports the highest loss obtained after a conventional CAF evaluation when varying the velocity direction φ in the interval $[0, \pi/2]$. This curve clearly shows that the maximum CPI allowed to avoid any migration effect for the considered case study is shorter than one-tenth of a second. Obviously, this limit would be slightly higher for medium speed targets. The blue curve is evaluated after correcting for a linear range migration (RM) only.
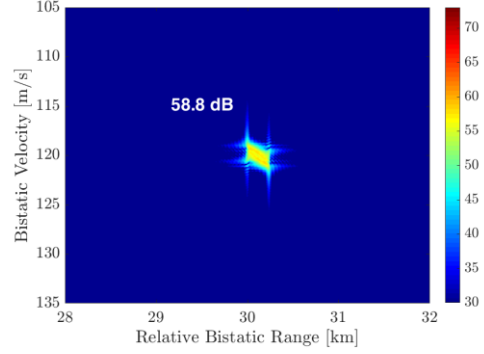

Fig. 1. Enlarged view of the bistatic range-velocity map obtained after a conventional CAF evaluation with $T = 2s$

By comparing the red and the blue curve we can conclude that in the considered application, due to the high bistatic range resolution offered by the DVB-T signal (approx. 40m), the need for compensating the linear range walk sets the tightest constraint to the CPI. Therefore, after the application of an appropriate Range Migration Compensation (RMC) stage, the CPI can be extended up to 0.3-0.4 s. Then the Doppler migration effects become prevalent for targets moving at constant velocity along the cross-range direction. Notice that the limit above is quite tight in the considered case study due to the vicinity of the target to the receiver and the IO positions.

Aiming at further increasing the CPI, at least the linear Doppler walk must be taken into account and compensated for (see the black curve). This additional processing stage theoretically allows to extent the CPI up to a few seconds where other migration effects appear due to higher order terms both in the range and Doppler variation laws. Nevertheless, the new bound on the CPI is typically well beyond the employable values. In fact, in the considered case study, a loss of approx. 0.5 dB is obtained for $T = 4s$. However, we observe that for the same target the limit to the CPI would be provided by the capability to resolve different scatterers constituting the target thus forming cross-range profiles [11]. In such a case, a hybrid coherent/non-coherent integration strategy would be preferable.
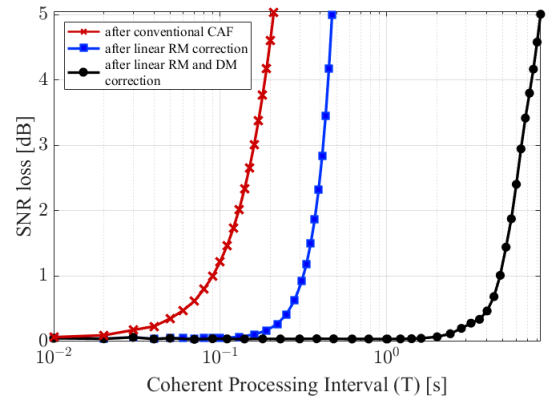

Fig. 2. SNR loss versus the coherent processing interval.

Ultimately, on the one hand, Fig. 2 proves that one must properly correct the linear range and Doppler walks when increasing the CPI over the tight limit $\overline{T}$. On the other hand, it demonstrates that a processing strategy able to effectively compensate for these first two migration effects would be sufficient and would allow the CPI to be extended up to a few seconds in the considered application against targets moving at constant velocity. The considerations above are at the basis of the two detection schemes proposed in this paper as described in the following Section.

III. PROPOSED DETECTION STRATEGIES

Both the proposed detection strategies rely on three subsequent processing stages applied after the stationary disturbance cancellation has been performed, as sketched in Fig.3.

With reference to the first block, namely the range compression stage, we resort to a batches approach [2] in order to recreate the classical slow-time/fast-time framework of a pulsed radar operating at a given pulse repetition frequency (PRF). Then, the RMC is based on efficient implementation of the Keystone Transform (KT) [10] using Lagrange P-order polynomial interpolation. We recall that, as shown in [8], the selection of the tuning parameters for the aforementioned sub-algorithms, namely the batch duration and the polynomial order P, is the result of a trade-off between the computational load and the SNR loss. A list of sub-algorithms included in each block and their tuning parameters is reported in Table I.

With reference to the same case study considered in Fig. 1, we report in Fig.4 the result after the range walk effect has been compensated with a 1-LPI based KT and batches of 1715 samples each. It is evident that the target now is focused in the range dimension and a SNR improvement on the measured peak is obtained with respect to the conventional CAF. However, the target response is still smeared in the Doppler dimension, with a SNR loss of approx. 5.9 dB with respect to the maximum expected coherent integration gain (72.58dB), confirming that a DM compensation stage is necessary.

Following the RMC stage, the DM can be corrected at each range cell r, operating on the RM compensated data in the slow-time domain, $x[r,m]$. For a given Doppler rate α, the sought correction is obtained by compensating for the corresponding parabolic phase law and then FFT-transforming the resulting sequence to synthetize the Doppler frequency domain:
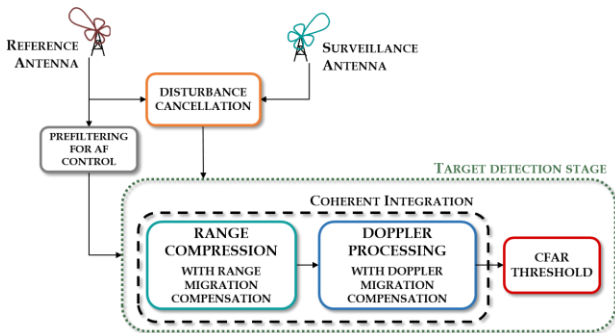
$$\chi[r,d] = \text{FFT}\left\{ x[r,m]e^{-j\frac{\pi}{\lambda \cdot PRF^2}\alpha m^2}, m = 0, \dots, M-1 \right\} \quad (1)$$

Since at the detection stage the target Doppler rate is unknown, a bank of filters is exploited for an appropriate set of Doppler rate values. In detail, we consider a grid of N_α Doppler rate values $\{\alpha_0, \dots, \alpha_{N_\alpha - 1}\}$, spaced by $\delta\alpha = \frac{\lambda}{T^2}$ (where λ is the wavelength), according to the depth of focus criterion.

We collect the 2D outputs of (1) obtained for different values of α in a 3D array $X[r,d,n]$, $r = 0, \dots, N_R - 1$, $d = 0, \dots, N_D - 1$, $n = 0, \dots N_\alpha - 1$, where N_R and N_D are the array extensions in the bistatic range and Doppler dimension, respectively. Following the Range and the Doppler Migration Compensation (RDMC) stages, two different detection schemes are then obtained based on alternative search strategies across the 3D (range, Doppler, Doppler rate) space.

A. Range-Doppler domain - based Search strategy (RDMC- RDS)

The first detection strategy, referred to as Range-Doppler domain - based search strategy (RDMC - RDS), looks for targets at each bin of the bistatic range - Doppler map.
To this purpose, a 2D map is built starting from the 3D array $X[r,d,n]$ by maximizing its intensity across the Doppler rate dimension, separately at each range-Doppler bin:

$$y[r,d] = \max_n \{ \|X[r,d,n]\|^2 \} \quad (2)$$

Afterwards, a 2D Cell Average- Constant False Alarm Rate (CA – CFAR) scheme is applied to detect potential targets. In particular, for a given cell under test (CUT) at range bin r_0 and Doppler bin d_0, namely $y[r_0, d_0]$, we define a set $I_{[r_0,d_0]}$ of M indices that identify proper range-Doppler bins surrounding the CUT ($y[r_m, d_m]$, $m \in I_{[r_0,d_0]}$, $|I_{[r_0,d_0]}| = \text{M}$). The average intensity estimated over these M secondary bins is used to scale the threshold:

$$y[r_0, d_0] \underset{H_0}{\overset{H_1}{\gtrless}} \lambda_{\text{RDS}} \left[\frac{1}{M} \sum_{m \in I_{[r_0,d_0]}} y[r_m, d_m] \right] \quad (3)$$

where the λ_{RDS} is properly set to take into account the disturbance statistics transformations resulting from the previous (non-linear) operations.

Fig. 3. Processing scheme for DVB-T PCLsystem exploting long coherent integraton times

TABLE I
SUMMARY OF SUB-ALGORITHMS AND TUNING PARAMETERS

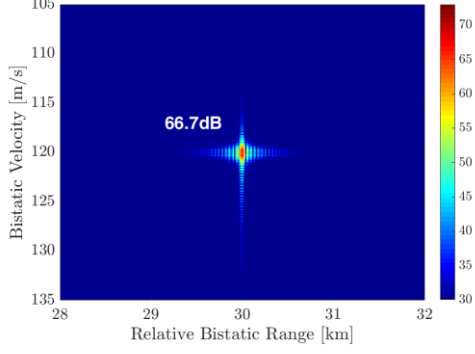| Processing Stage	List of Sub-Algorithms	Tuning Parameters
Prefiltering for AF control	Residual peaks removal and pilot equalization [13]	–
Disturbance Cancellation	Extensive Cancellation Algorithm [12]	Number of taps *1000 (~33 km)*
Range Compression with RMC	• Batches Algorithm[2] • P-LPI based Keystone Transform [8]	• Batch duration *1715 samples* • Polynomial order $P = 1$

Fig. 4. Enlarged view of the bistatic range-velocity map obtained after RMC with T=2s
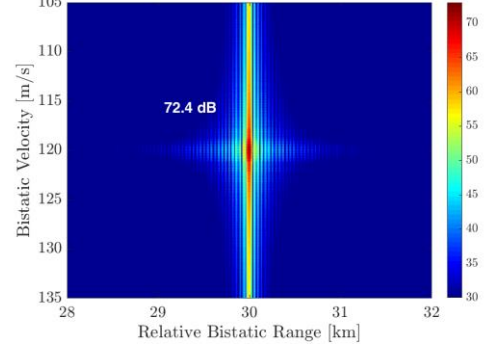

Fig. 5. Enlarged view of the 2D map after RDMC - RDS with T=2s

In Fig. 5 the 2D bistatic range-Doppler map after (2) is reported for the same case study shown in Fig. 1 and Fig.4. We notice that now the target peak is well focused in both range and Doppler dimension at the expected bin, with a gain of 5.7 dB with respect to Fig.4 and a negligible loss with respect to the maximum expected coherent integration gain (72.58dB). However, being the maximization in (2) performed on every bin, also the target sidelobes are maximized and their level is increased. This is especially evident in the Doppler dimension and must be taken into account when selecting the set of indices $I_{[r_0,d_0]}$ to be exploited as secondary data.

B. Range domain-based Search strategy (RDMC - RS)

The second approach, referred to as Range domain - based Search strategy (RDMC - RS), is based on the simplifying assumption that maximum one target is present at each range cell. The latter hypothesis is not unlikely to be verified when exploiting the DVB-T signals as source of opportunity, due to its fine bistatic range resolution.

To this aim, at each range bin of the 3D array $X[r, d, n]$, we perform a maximization of its square modulus across both Doppler and Doppler rate dimensions.

$$y[r] = \max_{d,n}\{ \|X[r, d, n]\|^2 \} \qquad (4)$$

As a result, a 1D output is obtained that is fed as input to the thresholding stage. A 1D CA-CFAR detection scheme can then be applied across the range dimension. In this case, differently from the RDMC-RDS, the disturbance power level P_D at the CUT is estimated over M range bins not necessarily adjacent to the CUT but rather collected from the farthest range bins included in $y[r]$. This is due to the fact that the latter contains all the maximized contributions at different range cells thus it is likely to include, at each range cell, non-negligible target contributions and/or clutter residuals that will not be representative of the disturbance affecting the CUT. Therefore, this results in comparing the CUT with a fixed threshold $\lambda_{RS} \cdot P_D$, being λ_{RS} properly modified to take into account the disturbance statistics transformations required by this second scheme.
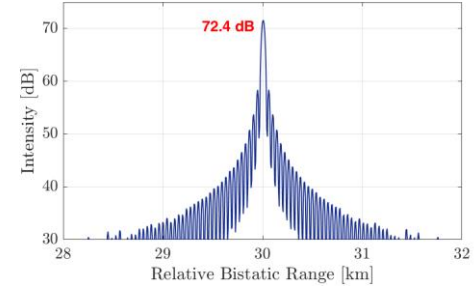

Fig. 6. 1D output of (5) obtained after RDMC - RS with T=2s

In Fig. 6, the 1D output of the RDMC - RS is reported. We notice that the target peak value coincides with that obtained in Fig. 5 and it is comparable with the maximum expected coherent integration gain (72.58dB).

IV. EXPERIMENTAL VALIDATION

In this Section, we investigate the benefits of the proposed strategies on real data, provided by Leonardo S.p.A. The acquisition geometry is sketched in Fig.7. Two Yagi-Uda antennas were employed, one steered toward the DVB-T transmitter of Monte Cavo (approx. 22.5 km away from the receiver site) was used as reference antenna, while the other was steered toward the surveillance area.

A. Acquisition campaign and data collection

An experimental campaign was carried out in April 2018 at Pratica di Mare Airport (Rome), using the DVB-T based AULOS passive sensor.

The latter was pointed at 310° clockwise from the north, with a main beam width of approx. 36°, in order to include in the main beam most of the civilian air traffic departing or arriving at Fiumicino airport. The DVB-T channel at carrier frequencies 570 MHz was exploited. In this paper, we consider a dataset composed of 25 sequential data files, each of 3.5s and spaced by approx. 9.8s, for a total acquisition time duration of approx. 245s.

Fig. 7. Acquisition geometry

Live Air Traffic Control (ATC) registrations of the aircrafts present in the same area have also been collected. The availability of air-truth for the non-cooperative targets allowed us to carry out a comparative analysis to evaluate the performance improvement. The entire dataset has been processed according to the DVB-T PCL processing scheme sketched in Fig.3 and the tuning parameters reported in Table I . Specifically, the removal of the undesired contributions in the surveillance channels, i.e. direct signal, clutter and multipath echoes, is performed via the Extensive Cancellation Algorithm (ECA) [12] over a range of 33 km. Then, the reference signal and the output signals from the ECA filter are exploited in order to evaluate the bistatic range/velocity map. In detail, a properly filtered reference signal is adopted in order to remove the high side-lobes and spurious peaks appearing in the DVB-T signal ambiguity function. To this purpose, we use the approach proposed in [13].

Successively, different algorithms have been employed and compared: the conventional CAF (no compensation case), the 1-LPI based KT (for the solely RMC stage) and the proposed detection schemes including both range and Doppler migration compensation, i.e. the RDCM-RDS and the RDCM-RS. The corresponding CFAR thresholds are set to achieve a nominal probability of false alarm equal to $P_{FA} = 10^{-6}$. In this work, the thresholds to be used (λ_{RDS} and λ_{RS}) have been found via Monte-Carlo simulation and verified in order to guarantee the desired P_{FA}.

B. Target detection performance analysis

Fig. 8 reports the raw detection results, obtained with the four approaches, using $T = 2s$. In each figure, in black we report the air-truth while the grey dots represents all the raw detections of the passive sensor within the total acquisition time; these might correspond to target returns, multipath/clutter residuals or false alarms. Eventually, the red dots represents the correct target detections, namely the detections that correlates with the available air-truth. By observing Fig. 8 we notice that:

- Target detection based on a conventional CAF approach (Fig. 8 (a)) yields continuous coverage only at distances up to a few tens of kilometres. Few additional detections or discontinuous plot sequences are obtained at higher distances, but they would not result in a track initialization.

- The solely RMC stage (Fig. 8 (b)) is able to substantially improve the target detection capability, especially for targets that move with a predominant radial velocity component. Targets characterized by this type of motion are also detected with good continuity at high bistatic ranges, , up to 250 km. However, some detections for targets moving with non-negligible tangential velocity are missing. This is particularly evident in the target tracks at approx. 160 km that rapidly cross the zero-Doppler. Notice that this is the typical trajectory of aircrafts landing at Fiumicino Airport.

- When performing the entire processing scheme described in Section III and sketched in Fig.3 a number of additional detections is obtained, especially for targets moving with cross-radial velocity. An illustrative example is identified by the green arrows in Fig. 8 (c-d) that show the additional plots obtained on the target track rapidly crossing the zero-Doppler at approx. 160 km with respect to Fig. 8(b). However, notice that the improvement is not tremendous due to the limited number of targets of opportunity that follow the aforementioned trajectory in the considered data files.

- The best performance is obtained when target detection is performed according to the RDMC – RDS strategy (Fig. 8 (c)). In fact, in this case, many additional plots are correcly detected. However, as noticed in Fig. 5, also target sidelobes are maximized and it is not unlikely for them to result in additional detections.

- The RDMC – RS strategy (Fig. 8 (d)) provides similar performance with just a few missing detections. These may be due to strong targets or clutter residuals appearing in the same range cell of a target of interest, which condition basically denies the fundamental assumption made for this search strategy. However, at the same time, we obtain a significant reduction in number of false alarms. In fact, since the number of decisions taken by the detector is reduced in this case due to the fact that the detection strategy is based on a 1D (range only) search, a lower amount of false alarms is obtained even operating with the same P_{FA} as in Fig. 8 (a-c). In fact, Fig. 8 (d) shows that almost all plots are correct detections and it is evident that this considerably simplifies the following tracking stage.

In conclusion, depending on the considered application, both the proposed strategies can be applied and effectively improve the target detection performance allowing the CPI to be extended up to a few seconds. Specifically, thanks to its flexibility and capability to possibly detect targets at each range-Doppler bin, the RDMC-RDS is particularly useful in high traffic density scenarios, such as short-range surveillance applications. In contrast, the RDMC-RS could be a solution in long-range surveillance applications, where the simplifying assumption of having maximum one target at each range bin is very likely to be verified. Obviously, a hybrid version of the two techniques could be exploited by partitioning the search region into two or more bistatic velocity regions (e.g. one for positive and one for negative bistatic velocities) where the RDMC-RS can be applied thus allowing the possibility to detect multiple targets per each range cell.
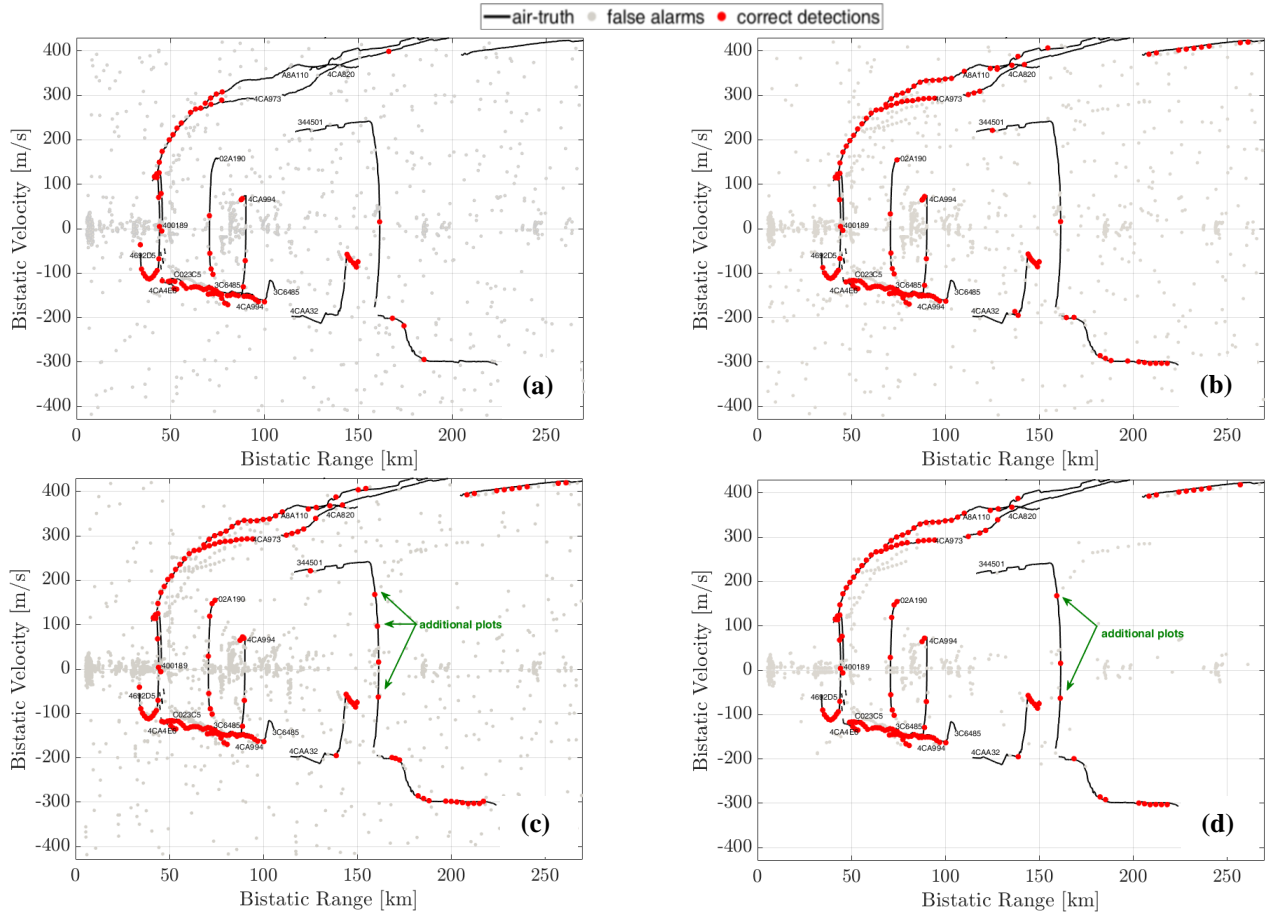
Fig. 8. Detection results, using T = 2s, $P_{FA} = 10^{-6}$ and: (a) Conventional CAF s; (b) only RMC; (c) RDMC - RDS; (d) RDMC - RS

V. CONCLUSIONS

In this paper, we exploited long coherent integration times in a DVB-T based passive radar system for air traffic surveillance. In order to effectively benefit from the extended coherent integration, we proposed two target detection schemes able to correct the range and Doppler walk effects of the targets of interest thus improving the target detection capability while controlling the false alarm rate. We have shown, by means of application against both simulated and real data, that the two proposed approaches allow the coherent processing interval to be increased up to a few seconds thus significantly enhancing the coverage of the resulting system.

REFERENCES

[1] P.E., Howland, IEE Proc. Radar, Sonar and Navigation. (Special Issue on Passive Radar System), 152, 3, (June 2005).

[2] P. Lombardo and F. Colone: "Advanced processing methods for passive bistatic radar", in W.L.Melvin and J. A.Scheer (Eds):"Principles of Modern Radar: Advanced Radar Techniques", Raleigh,NC: SciTech Publishing, pp. 739–82, (2012).

[3] J. Palmer, H. Harms, S. Searle, L Davis, "DVB-T passive radar signal processing" *IEEE Trans.s on Signal Processing*, 2013, 61 (8), pp. 2116-2126.

[4] H. D., Griffiths,C. J. Baker, "Passive coherent location radar systems. Part 1: Performance prediction.", *IEE Proc.on RSN*, 2005,152, 3, pp. 153-159.

[5] J. M. Christiansen, K. E. Olsen and G. Weiß, "Coherent range and Doppler-walk compensation in PBR applications," *2014 15th International Radar Symposium (IRS)*, Gdansk, 2014, pp. 1-4.

[6] J. M. Christiansen and K. E. Olsen, "Range and Doppler walk in DVB-T based Passive Bistatic Radar," *2010 IEEE Radar Conference*, Washington, DC, 2010, pp. 620-626.

[7] M. Malanowski, K. Kulpa and K. E. Olsen, "Extending the integration time in DVB-T-based passive radar," *2011 8th European Radar Conference*, Manchester, 2011, pp. 190-193.

[8] F. Pignol, F. Colone and T. Martelli, "Lagrange-Polynomial-Interpolation-Based Keystone Transform for a Passive Radar," in *IEEE Trans. on AES,* vol. 54, no. 3, pp. 1151-1167, June 2018.

[9] T. Martelli, F. Filippini, F. Pignol, F. Colone and R. Cardinali, "Computationally effective range migration compensation in PCL systems for maritime surveillance," *2018 IEEE Radar Conference (RadarConf18)*, Oklahoma City, OK, 2018, pp. 1406-1411.

[10] K. M. Scott, W. C. Barott and B. Himed, "The keystone transform: Practical limits and extension to second order corrections," *2015 IEEE Radar Conference (RadarCon)*, Arlington, VA, 2015, pp. 1264-1269.

[11] F. Colone, D. Pastina and V. Marongiu, "VHF Cross-Range Profiling of Aerial Targets Via Passive ISAR: Signal Processing Schemes and Experimental Results," in *IEEE Transactions on Aerospace and Electronic Systems*, vol. 53, no. 1, pp. 218-235, Feb. 2017.

[12] F. Colone, D. W. O'Hagan, P. Lombardo and C. J. Baker, "A Multistage Processing Algorithm for Disturbance Removal and Target Detection in Passive Bistatic Radar," in IEEE Transactions on Aerospace and Electronic Systems, vol. 45, no. 2, pp. 698-722, April 2009.

[13] F. Colone, D. Langellotti, and P. Lombardo, "DVB-T signal ambiguity function control for passive radars," *in IEEE Transactions on Aerospace and Electronic Systems*, vol. 50, no. 1, pp. 329-347, January 2014.